

See discussions, stats, and author profiles for this publication at: <https://www.researchgate.net/publication/280747430>

# Cavitation Avoidance in Nitrous Oxide Rocket Engines Using the Efficient Transient 1D Downwind Prediction

Article in *Applied Mechanics and Materials* · October 2014

DOI: 10.4028/www.scientific.net/AMM.656.95

CITATIONS

0

READS

350

3 authors:



**Radu Dan Rugescu**

Polytechnic University of Bucharest

101 PUBLICATIONS 135 CITATIONS

[SEE PROFILE](#)



**Alina Bogoi**

Polytechnic University of Bucharest

13 PUBLICATIONS 2 CITATIONS

[SEE PROFILE](#)



**Constantinescu Cristian-Emil**

Polytechnic University of Bucharest

11 PUBLICATIONS 27 CITATIONS

[SEE PROFILE](#)

Some of the authors of this publication are also working on these related projects:



NERVA Launcher [View project](#)

## Cavitation avoidance in nitrous oxide rocket engines using the efficient TRANSIENT 1D downwind prediction

RUGESCU Radu Dan<sup>1, a \*</sup>, BOGOI Alina<sup>2, b</sup>  
and CONSTANTINESCU Emil Cristian<sup>2, c</sup>

<sup>1</sup>ADDA Ltd, 18 Bancila St, Bucharest 060144, Romania

<sup>2</sup>UPB, 1 Polizu St, Bucharest 011061, Romania

<sup>a</sup>rugescu@yahoo.com, <sup>b</sup>bogoi\_alina@yahoo.com, <sup>c</sup>constantinescu\_ce@yahoo.com

\*corresponding author

**Keywords:** cavitation, nitrous oxide, rocket engines, space propulsion, dual phase flow

**Abstract.** Nitrous oxide has recently entered violently the arena of space propulsion and gained interest, due to its high energy and gasification potential and despite its low oxygen content as an oxidizing chemical and its instability over some 600 C. However, its physical and chemical instability soon proved to be a potential hazard and led to a renewed interest in the study of its behavior as a fluid. In the present contribution computer simulation of the liquid phase flow of the nitrous oxide under high pressure is used to predict and avoid the cavitation into the feeding line tract of rocket engines, specifically of the compound rocket engines feeding line. The method involves a substantially simplified 1-D description of the fluid motion with sufficiently accurate determination of cavitation risk where the feeding duct suffers blunt variations of the cross area or steep turns and corners involving sensible static pressure variations of the fluid. A means of avoiding dangerous behaviors of the nitrous oxide is thus developed that could increase safety margins during the handling of this quite unpredictable oxidizer for the compound, combined or hybrid rocket engines.

### Introduction

Although nitrous oxide (N<sub>2</sub>O), first discovered in 1793 by the English scientist Joseph Priestly, is known as a convenient curing means in medicine [1, 2] and often used for more than two hundred years as an anesthetic [3, 4], with recent extension in the area of maternal care [5], little was known in fact on its challenging behavior and detonation potential, disastrously demonstrated in the 2007 accident at Scaled Composites Co. on an county airport near Los Angeles, US [6]. The fact that no specific cause of the accident could have been found during the official investigation [7] leaves open the question of safety procedures with N<sub>2</sub>O handling. Since no hazard have been ever found to develop with N<sub>2</sub>O in liquid phase, a series of potential causes were considered as potential hazards for N<sub>2</sub>O handling, including contamination with organic soot, local overheating due to diverse causes, leading to a local vaporization and formation of bubbles, in fact a sort of static cavitation, the sudden opening of valves that produces a pressure transient with bubble formation, local catalytic effects due to the presence on unsuitable materials in the plumbing etc. [8, 9]. One of the most subtle causes which are suspected for the apparently irregular detonation of this substance is the sudden dynamic cavitation that could develop into the transfer feed line during the liquid flow for tank feeling procedure [10].

Cavitation is commonly associated to the rotating machines with blades, where a reduced pressure would develop around the convex part of their profile and leads to local vaporization due to the liquid instant boiling [11-14]. The same effect is producing however around any sudden variation of the area/shape of the duct where the instable liquid is flowing and the main target of the contribution of the authors is to identify this potential hazard along the feed line of the experimental compound motor MEC-80 developed by ADDA.

### Euler type transient equations

In order to focus the research on the transient variation of the static pressure in the fluid as a response to variations in the cross area and shape of the duct the viscous effects in the fluid are considered insignificant and the fluid is assessed as an ideal, incompressible, non-viscous and non-vaporizing liquid. However, the fast transients produced at flow startup and shut down are important and are thus considered into the computational model that has the known 3-D form

$$\nabla \cdot \mathbf{V} = 0, \quad \frac{d\mathbf{V}}{dt} = \mathbf{F} - \frac{1}{\rho} \nabla p, \quad (1)$$

used directly in the form (2) for the one-directional motion,

$$\begin{aligned} \frac{\partial u}{\partial x} &= -u \frac{d \ln A}{dx}, \\ \frac{\partial u}{\partial t} + u \frac{\partial u}{\partial x} + \frac{1}{\rho} \frac{\partial p}{\partial y} &= 0, \end{aligned} \quad (2)$$

or in the generalized [17] Chorin's 2-D pseudo-compressibility form,

$$\begin{aligned} \frac{1}{\beta^2} \frac{\partial p}{\partial t} + \frac{\partial u}{\partial x} + \frac{\partial v}{\partial y} &= 0, \\ \frac{u}{\beta^2} \frac{\partial p}{\partial t} + \frac{\partial u}{\partial t} + u \frac{\partial u}{\partial x} + v \frac{\partial u}{\partial y} + \frac{\partial p}{\partial x} &= 0, \\ \frac{v}{\beta^2} \frac{\partial p}{\partial t} + \frac{\partial v}{\partial t} + u \frac{\partial v}{\partial x} + v \frac{\partial v}{\partial y} + \frac{\partial p}{\partial y} &= 0 \end{aligned} \quad (3)$$

both for negligible field forces  $\mathbf{F}=0$ . The latter also transforms, for the one-directional case applicable to slender duct flows, into the 1-D basic equations of mass and impulse conservation of the dependent state variables *speed* and *pressure*,

$$\begin{aligned} \frac{1}{\beta^2} \frac{\partial p}{\partial t} - u \frac{d \ln A}{dx} &= 0, \\ \frac{\partial u}{\partial t} + u \frac{\partial u}{\partial x} + \frac{\partial p}{\partial x} + u \frac{d \ln A}{dx} &= 0, \end{aligned} \quad (4)$$

where the physical conditions are given as  $\rho = \text{const.}$ ,  $A(x) = \text{given}$ .

According to recommendations in [16] the constant value for  $\beta$  should be around  $\tilde{u}$ . The cavitation and the subsequent two phase flow that accompanies cavitation is still considered as ineffective, in order to arrive at the conditions for local vaporization first. The main problem in this case is the accommodation of the one-directional motion concept with local variations in the cross section size of the duct and with the blunt turns that appear at duct corners.

### The two-point boundary value problem of the controlled duct

When the application is focused on the computation of pressure distribution along a given pipe with a given profile of the cross area and given pressure values at both ends of the open duct, the problem resides in the computation of the velocity and pressure distribution in time along the whole duct, in compliance with the given and constant values of the pressure at the two end openings.

Although the inviscid-incompressible flow into the duct is governed by that simple description in (2) the flow rate and local velocities that accomplish this flow rate are not known ab initio. The problem enters the area of the two-point boundary value problems and the initial ( $t=0$ ) distribution of velocity and pressure values along the pipe must first be computed.

The specific given data of the problem are:

- a) the size and profile of the duct in the form of the cross area distribution  $A(x)$  along the pipe;
- b) the given values of the pressure at both ends of the pipe  $p_1$  and  $p_N$ ;
- c) the given value of the liquid constant density  $\rho$ .

Nothing else is known of the flow.

As far as the liquid is incompressible, at every instant in time the flow rate, that means both volume and mass flow rates, are absolute constants along the pipe and this gives the possibility to build the velocity distribution along the pipe when the flow rate is known. But it isn't. Following the physical phenomenon, when a control valve is opened at the downwind end of the pipe a continuous flow of liquid starts to be displaced along the pipe due to the pressure head and this mass of liquid gradually accelerates until the pressure values at both ends equal the imposed pressure values (b) of the system.

In order to model this type of flow a numerical scheme is conceived based on the finite, constant difference computational mesh as informally presented in Fig. 1. A finite difference algorithm is then attached to this mesh in order to approximate the continuous flow with the discontinuous replacer that will be forced to reproduce the real flow with the desired accuracy, by transforming the partial derivatives equations (2) or (4) into a finite difference form convenient for direct computations from node to node in the mesh.

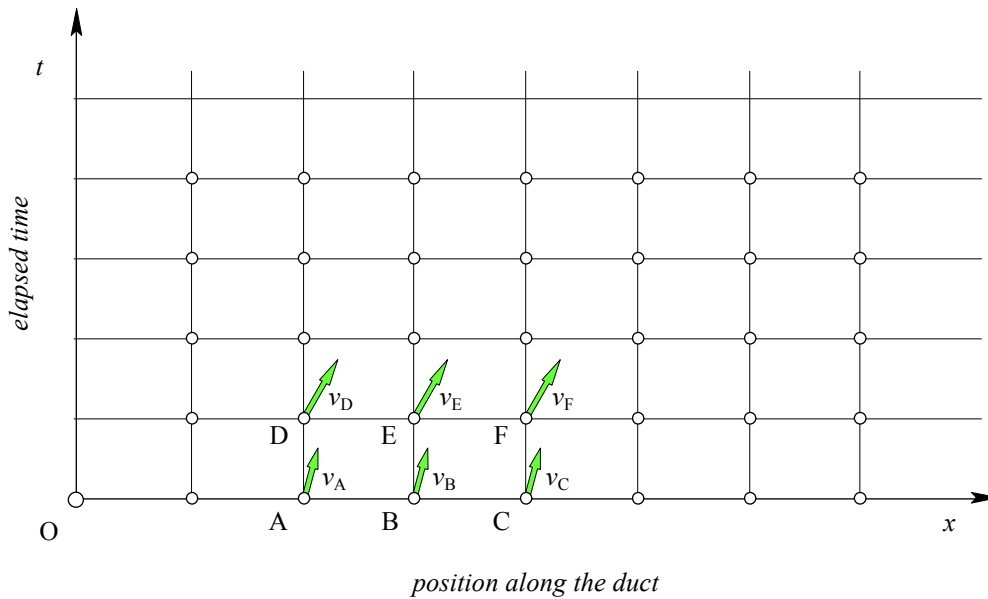


Fig. 1. Equi-positioned computational mesh into the real  $\{t-x\}$  plane.

The given problem is permeable to an indirectly implicit, finite difference algorithm that replaces the continuous equations (4) with their working form (5), according to Fig. 1,

$$\frac{p_D - p_A}{t_D - t_A} = \beta^2 \frac{u_A}{A_A} \frac{A_B - A_A}{x_B - x_A},$$

$$\frac{u_D - u_A}{t_D - t_A} + u_A \frac{u_B - u_A}{x_B - x_A} + \frac{p_B - p_A}{x_B - x_A} = - \frac{u_A}{A_A} \frac{A_B - A_A}{x_B - x_A}, \tag{5}$$

where the formulae are to be gradually applied along the initial row of nodes established on the abscise axis. Equations (5) are only written for the initial time value ( $t=0$ ) in the given form.

However, this computational working form has the disadvantage of simultaneously involving too many increments in the dependent variables and this is why the more useful form is the transcription obtained by extending the equations from the form (5) into

$$\begin{aligned} \frac{u_B - u_A}{x_B - x_A} &= -\frac{u_A}{A_A} \frac{A_B - A_A}{x_B - x_A}, \\ \frac{p_D - p_A}{t_D - t_A} &= \beta^2 \frac{u_A}{A_A} \frac{A_B - A_A}{x_B - x_A}, \\ \frac{u_D - u_A}{t_D - t_A} &= \frac{v_A^2}{A_A} \frac{A_B - A_A}{x_B - x_A} - \frac{1}{\rho} \frac{p_B - p_A}{x_B - x_A}. \end{aligned} \quad (6)$$

For a quasi-viscous flow the pressure increment along the abscise axis could be rebuilt from the function  $\varphi^{n+1}$  through the relationship [18], as suggested by [16]

$$p^{n+1} = \varphi^{n+1} \frac{\Delta t}{2Re} \nabla^2 \varphi^{n+1}. \quad (7)$$

In order to compute  $\varphi^{n+1}$  the Poisson equation is used [19]

$$\nabla^2 \varphi^{n+1} = \frac{\nabla \cdot u^*}{\Delta t}. \quad (8)$$

For the inviscid case however the pressure gradient along the direction of motion is only related to the variation in cross area values of the duct, as seen from the second equation in (6). The following computational steps are then used.

Stage I. A steady state value of the flow rate  $Q_{st} \equiv A_m v_0$  is first obtained from the global static pressure difference ( $p_1 - p_N$ ) and the mean cross area of the duct  $A_m$ , using the Bernoulli equation of energy in integral form,

$$Q_{st} = A_m \sqrt{\frac{2(p_1 - p_N)}{\rho}}, \quad (7)$$

where the assumption was made that the entrance in the pipe is at rest (entrance from a large tank). In the absence of viscosity no frictional losses are present and at a constant diameter of the pipe the pressure does not vary along the duct. The first numerical value of the fluid velocity at the entrance of the tube is thus given by

$$v_{0,1} = Q_{st} / A_1, \quad (8)$$

Extending equations (6) to the entire computational mesh the following solving system appears

$$\begin{aligned} \frac{u_{i,j+1} - u_{i,j}}{x_{i,j+1} - x_{i,j}} &= -\frac{u_{i,j}}{A_{i,j}} \frac{A_{i,j+1} - A_{i,j}}{x_{i,j+1} - x_{i,j}}, \quad \frac{p_{i+1,j} - p_{i,j}}{t_{i+1,j} - t_{i,j}} = \beta^2 \frac{u_{i,j}}{A_{i,j}} \frac{A_B - A_{i,j}}{x_B - x_{i,j}}, \\ \frac{u_{i+1,j} - u_{i,j}}{t_{i+1,j} - t_{i,j}} &= \frac{v_{i,j}^2}{A_{i,j}} \frac{A_{i,j+1} - A_{i,j}}{x_{i,j+1} - x_{i,j}} - \frac{1}{\rho} \frac{p_{i,j+1} - p_{i,j}}{x_{i,j+1} - x_{i,j}}. \end{aligned} \quad (9)$$

Stage II. Starting from a given distribution of pressures along the pipe and successively applying the difference algorithm in (9) a new distribution of pressures and velocities develop along the pipe within a given time frame of the computation, up to the steady state. This values end in a different final pressure at the end of the pipe and a linearized correction is made to obtain the desired fit of the given end-value pressure. The process is repeated to the desired accuracy.

### Numerical results for a given configuration

The following configuration given in Fig. 2 and resulting from the design of the feed system of the compound rocket engine MEC-80JMIC was subjected to the method here presented.

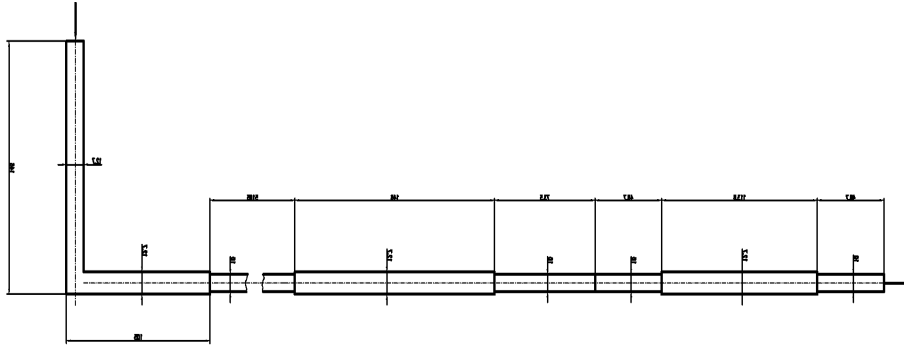


Fig. 2. The design configuration of the duct.

The variation of the pressure along the given pipe as resulting after 27 time steps is shown in Fig. 3. It reveals the presence of pressure raises and drops at the stages where cross area variations of the duct are visible.

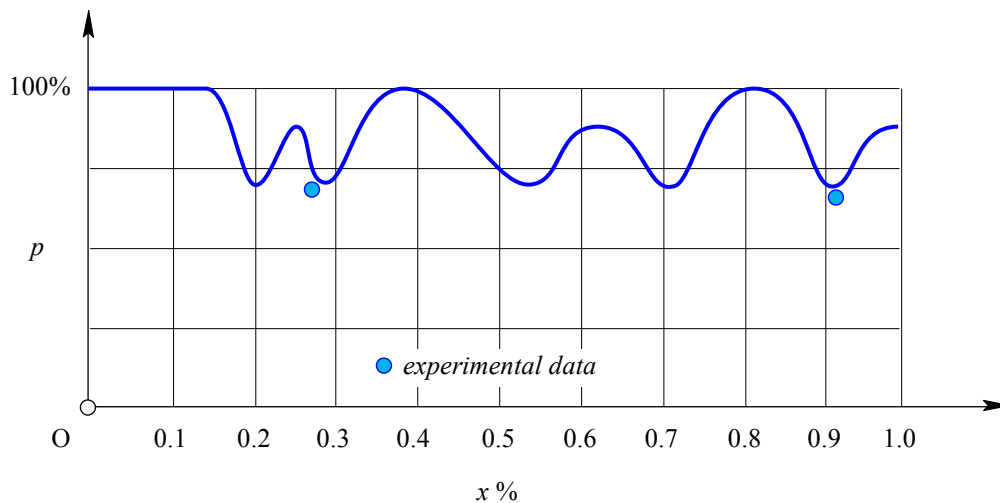


Fig. 3. Smoothed computed pressure distribution along the pipe and experiments.

These variations have to be compared with the admissible variations of the liquid phase of the fluid in order to establish the limits of vaporization at the given temperature. This aspect is specific to the fluid and for the present application is characteristic to the nitrous oxide subjected to tests.

### Conclusion

The transient numerical method allows predicting the pressure distribution along a given length pipe fast and easy. The results are in good agreement with the experimental measurements in the set.

**References**

- [1] Amort, Dr. Robert, The Physiological Action of Nitrous Oxide, *New York Medical Journal*, August, 1870.
- [2] I. O'Sullivan, and J. Bengler, Nitrous oxide in emergency medicine, *Emerg. Med. J.*, May 2003; 20(3), 214–217.
- [3] Johnson, Dr. George, A Lecture on the Physiology of Coma and Anaesthesia, *Medical Times and Gazette*, April 3, 1869.
- [4] Ruben, H., Nitrous oxide analgesia in dentistry. Its use during 15 years in Denmark, *Br. Dent. J.*, 1972 Mar 7, 132(5), 195–196.
- [5] Rosen, M. A., Nitrous oxide for relief of labor pain: a systematic review, *Am. J. Obstet. Gynecol.* May 2002, 186(5 Suppl Nature), 110-126.
- [6] Abdollah Tami, and Stuart Silversteine, Test site explosion kills three, *Los Angeles Times*, 27 July 2007.
- [7] \*\*\*, *Inspection Report No. 0950625 at Scaled Composites, LLC*, OSHA Report, 2007.
- [8] B. Berger, *Is nitrous oxide safe?* Swiss Propulsion Laboratory, 2007.
- [9] \*\*\*, Scaled Composites accident - Mojave Desert, California, Observations and comments on Cal/OSHA report Knights Arrow, <http://www.knightsarrow.com/rockets/scaled-composites-accident/>, 2014.
- [10] N. Tiliakos, J. S. Tyll, R. Herdy, D. Sharp, M. Moser, and N. Smith, Development and testing of a nitrous oxide/propane rocket engine, *37th Joint AIAA/ASME/SAE/ASEE Propulsion Conference and Exhibit*, 8-11 July 2001, Salt Lake City, Utah US.
- [11] S. Khurana, Navtej and Hardeep Singh, Effect of cavitation on hydraulic turbines - A review, *International Journal of Current Engineering and Technology*, Vol.2, No.1 (March 2012), ISSN 2277–4106.
- [12] Escaler, Xavier, Egusquiza, Ed., Farhat, Mohamed, Avellan, Francois, and Coussirat, Miguel, Detection of cavitation in hydraulic turbines, *Mechanical Systems and Signal Processing*, Vol. 20, Issue 4, May 2006, 983-1007.
- [13] Knapp, R.T., Daili, J.W., and Hammit, F. G., *Cavitation*, New York, Mc Graw Hill Book Company, 1970, 578p.
- [14] Terentiev, A., Kirschner, I., and Uhlman, J., *The Hydrodynamics of Cavitating Flows*, Backbone Publishing Company, 2011, 598pp.
- [15] Peyret, Roger (ed), *Handbook of Computational Fluid Mechanics*, Academic Press, 25 Mar. 1996, 467 pag.
- [16] Turkel, E., Fiterman, A., and B. Van Leer, Preconditioning and the Limit to the Incompressible Flow Equations, ICASE Report No. 93-42, Langley Research Center, Hampton Virginia, USA 1993.
- [17] Chorin, A. J., A Numerical Method for Solving Incompressible Viscous Flow Problems, *Journal of Computational Physics*, 2 (1967), pp. 12-26.
- [18] Lee, Long, *A class of high-resolution algorithms for incompressible flows*, Department of Mathematics, University of Wyoming, Laramie, WY 82071, USA, 2010.
- [19] D. Brown, R. Cortez, and M. L. Minion. Accurate projection methods for the incompressible Navier-Stokes equations, *J. Comput. Phys.*, **168**, 2001, 464-499.

**Monitoring, Controlling and Architecture of Cyber Physical Systems**

10.4028/www.scientific.net/AMM.656

**Cavitation Avoidance in Nitrous Oxide Rocket Engines Using the Efficient Transient 1D Downwind Prediction**

10.4028/www.scientific.net/AMM.656.95